Impact of an M3D-C1 modeled plasma response on simulations of the DIII-D plasma edge with EMC3-EIRENE

H. Frerichs[1,2], O.Schmitz[1,2], D. Reiter[1], T.E. Evans[3], Y. Feng[4], N.M. Ferraro[3]

[1] *Institute for Energy and Climate Research IEK-4, Jülich GmbH, 52425 Jülich, Germany*

[2] *University of Wisconsin - Madison, Department for Engineering Physics, Madison, WI, USA*

[3] *General Atomics, P.O. Box 85608, San Diego, California 92186-5608, USA*

[4] *Max Planck Institut für Plasmaphysik, IPP-EURATOM Association, Greifswald, Germany*

Introduction

Modeling of the impact of resonant magnetic perturbations (RMPs) on the plasma edge is a key topic for the analysis of present experiments and the design of future magnetic fusion reactors. In particular since the recent success of RMPs to control edge localized instabilities (ELMs), they are considered to be essential for the successful operation of the next step fusion device ITER [1]. The EMC3-EIRENE code is a three-dimensional transport solver for the edge plasma interacting with neutral gas [2]. A key ingredient for this tool is a magnetic field aligned grid, which allows a fast reconstruction of magnetic field lines [3]. The geometric setup is flexible enough to allow complex magnetic field structures including short magnetic flux tubes as well as chaotic regions with long wall-to-wall field line connection length. However, because the field aligned grid has to be generated in a first step and then provided to the transport solver, it does not take into account the feedback (response) from the plasma to the magnetic field. While the majority of the simulations that have been performed in the past are based on the so-called vacuum-approach (i.e. a superposition of the vacuum RMP field and the underlying magnetic equilibrium), we have recently begun to estimate the impact of a plasma response [4]. These first estimates are based on the assumption of screening of certain resonant modes close to the separatrix. In the present contribution we take into account the plasma response taken from a linear two-fluid MHD calculation with the M3D-C1 code [5], which has been implemented into the grid generator for the EMC3-EIRENE code.

Magnetic field configuration and other input

The magnetic field configuration is based on DIII-D discharge 148712 equilibrium at 4140 ms. This configuration is characterized by a toroidal magnetic field of $B_T = 1.96\,\mathrm{T}$ at the magnetic axis and a plasma current of $I_p = 1.59\,\mathrm{MA}$, resulting in an edge safety factor of $q_{95} = 3.55$. The RMP field is generated by the I-coils in $n = 3$ configuration with a coil current of $I_c = 4\,\mathrm{kA}$. The resulting magnetic field structure is shown in figure 1. A remarkable feature of this configuration

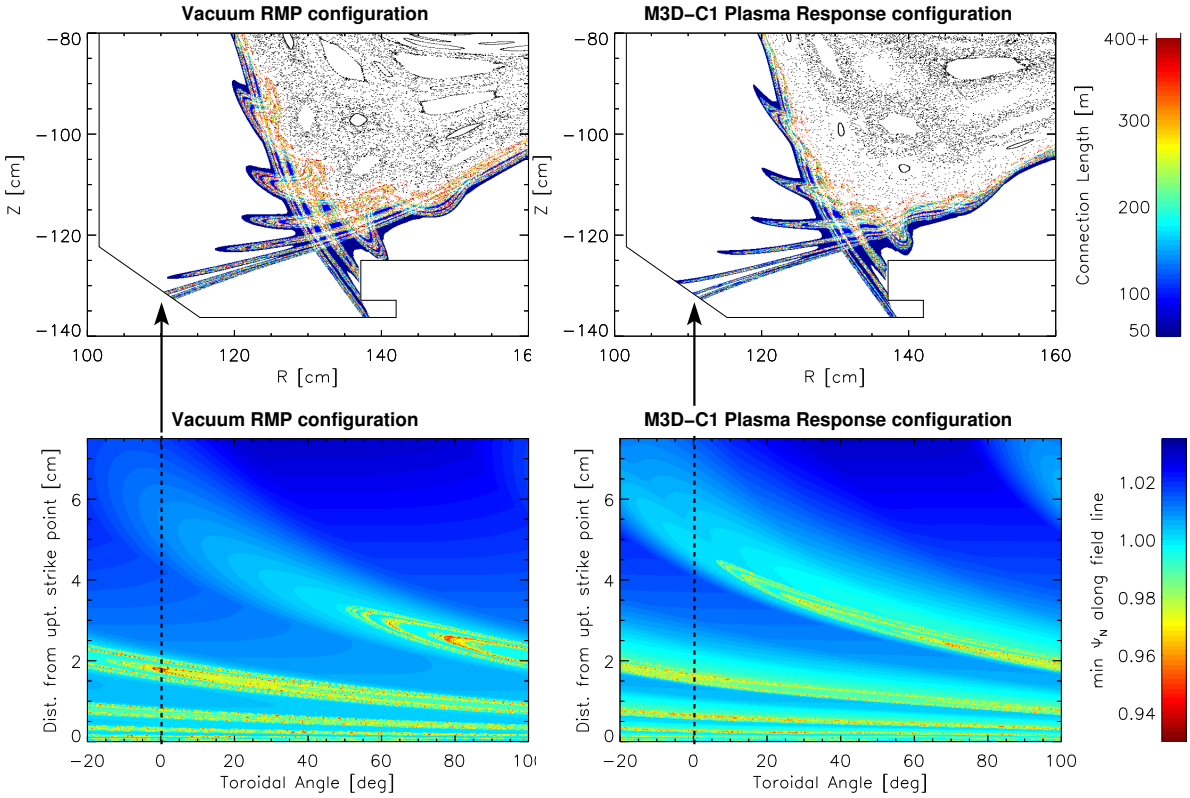

Figure 1: Magnetic field configuration of the vacuum RMP configuration and the M3D-C1 plasma resonse configuration: depicted by the connection length combined with a Poincaré plot at the X-point region and by the penetration depth of field lines (i.e. minimum of polidal flux Ψ along field line) at the inner strike point.

is that a linear two-fluid MHD modeling of the plasma response with the M3D-C1 code [5] results in a stretching of the helical lobes, which consequently leave a more elongated footprint at the divertor target than in the vacuum RMP configuration.

Boundary conditions and model parameters for transport simulations

The pumping efficiency is initially set to $\varepsilon_{\text{pump}} = 40\,\%$, which is consistent with conditions in the experiment (see [6] for details on neutral gas pumping in EMC3-EIRENE). A second pair of simulations is performed with $\varepsilon_{\text{pump}} = 4\,\%$, because we have recently shown that a significantly lower pumping efficiency allows to access divertor conditions which are closer to experimental observations [7]. The input power is set to $P_{\text{in}} = 2.7\,\text{MW}$, which is lower than in the experiment. We have chosen a lower value because earlier simulation results have indicated that some power loss channel exists in the experiment which are not present in the simulations. The level of anomalous cross-field transport is set to $D_\perp = 0.2\,\text{m}^2\,\text{s}^{-1}$ and $\chi_\perp = 0.6\,\text{m}^2\,\text{s}^{-1}$ consistent with earlier simulations for DIII-D, and the particle input rate is $\Gamma_{\text{in}} = 1.1 \cdot 10^{21}\,\text{s}^{-1}$.

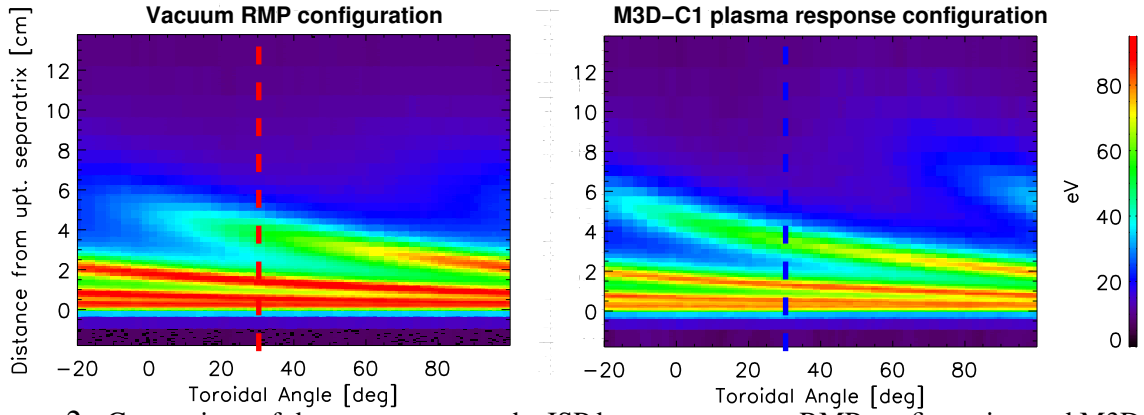

Figure 2: Comparison of the temperature at the ISP between vacuum RMP configuration and M3D-C1 plasma response configuration ($\varepsilon_{\text{pump}} = 40\,\%$).

Discussion of simulation results

The temperature at the ISP is shown in figure 2 for the $\varepsilon_{\text{pump}} = 40\,\%$ simulations. It can be seen that the striation pattern of the magnetic footprint is very well reflected in the temperature. A more quantitative comparison between the vacuum RMP and M3D-C1 plasma response configuration is given in figure 3 which demonstrates that both temperature and heat flux at the outermost peak are moderately increased if a plasma response is taken into account (due to the stretching of the helical lobes)! As reported earlier [7], recycling conditions can have a significant impact on the heat flux striation pattern. Access to high recycling conditions can be achieved numerically by reducing the pumping efficiency, and it is demonstrated in figure 3 that the outer heat flux peak disappears for $\varepsilon_{\text{pump}} = 4\,\%$ as a result of a significant temperature drop at that location (below a few eV). This result is seen for both vacuum RMP and M3D-C1 plasma response configurations. The peak heat flux under these conditions is of the order $2-3\,\text{MW}$ which is consistent with measurements. To characterize the recycling conditions in both simulation pairs we calculate the average temperature at the ISP T_d and compare it to the upstream quantity T_u. As the upstream location is not well-defined in the RMP configuration with its mix of long and short connection lengths to the divertor targets, we approximate T_u by taking the average temperature from the grid cells which are just inside the SOL-core block interface in the grid (see [8] for details on the grid structure). For the $\varepsilon_{\text{pump}} = 4\,\%$ simulations we get $T_d/T_u \approx 4-6\,\%$, i.e. a significant upstream-to-downstream temperature drop consistent with a high recycling regime. However, for the $\varepsilon_{\text{pump}} = 40\,\%$ simulations we get $T_d/T_u \approx 55-60\,\%$ which indicates that these simulations are in fact closer to a linear recycling regime. High recycling conditions allow a general agreement with measurements regarding the level and the striation pattern of the ISP heat flux, but for that we have to significantly deviate from the boundary conditions (P_{in}, $\varepsilon_{\text{pump}}$) given by the experiment.

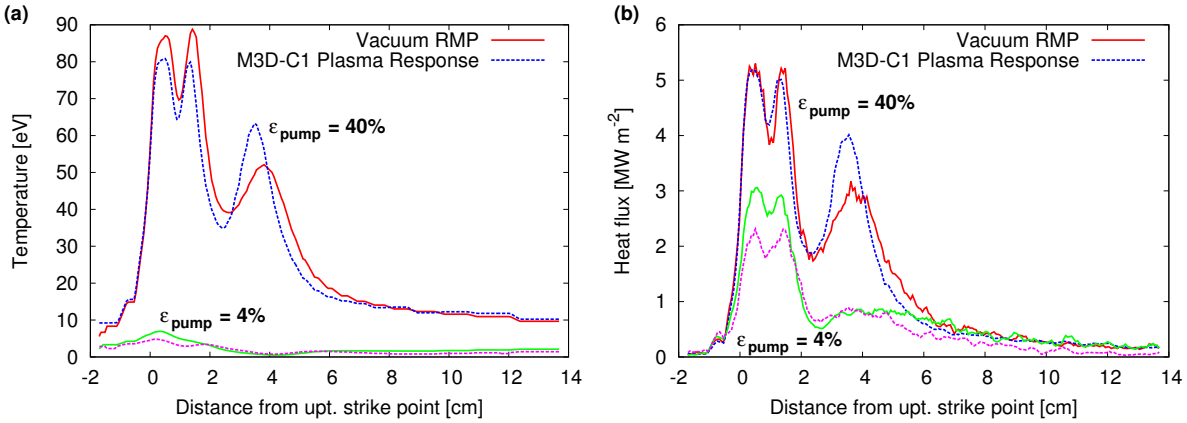

Figure 3: Profiles of (a) ISP target temperature and (b) heat flux for the vacuum RMP configuration (solid) and M3D-C1 plasma response configuration (dashed) at $\varphi = 30$ deg.

Conclusions

A comparison between a vacuum RMP and a plasma response configuration provided by the M3D-C1 code has demonstrated that even a stretching rather than a shrinking of the RMP induced helical lobe structure can occur. A corresponding modification (albeit a weak one) of the simulated edge plasma can be found. Other discharges can result in a larger impact of the plasma response and for those it would be more important to include these effects in edge plasma simulations. However, considering that we had to decrease the input power to get to reasonable values of the heat flux, and considering that we had to decrease the pumping efficiency to access high recycling conditions which exhibit the "missing outer heat flux peak" consistent with measurements, we conclude that presently the largest challenge for DIII-D edge plasma simulations is to get a better understanding of the steady state particle and energy throughput conditions in the experiment which are boundary conditions for the edge transport model.

Acknowledgements

This work was supported in part by the US Department of Energy under DE-FC02-04ER54698 and DE-FG02-95ER54309.

References

[1] Loarte A, *et al.*, 2014 *Nuclear Fusion* **54** 033007.
[2] Feng Y, *et al.*, 1999 *Journal of Nuclear Materials* **266-269** 812.
[3] Feng Y, *et al.*, 2005 *Phys. Plasmas* **12** 052505 1.
[4] Frerichs H, *et al.*, 2012 *Phys. Plasmas* **19** 052507.
[5] Ferraro N M, 2012 *Phys. Plasmas* **19** 056105.
[6] Frerichs H, *et al.*, 2012 *Nuclear Fusion* **52** 023001.
[7] Frerichs H, *et al.*, 2014 *Phys. Plasmas* **21** 020702.
[8] Frerichs H, *et al.*, 2010 *Comp. Phys. Commun.* **181** 61.